Diamine-Appended Mg$_2$(dobpdc) Nanorods as Phase-Change Fillers in Mixed-Matrix Membranes for Efficient CO$_2$/N$_2$ Separations

Lorenzo Maserati,[†] Stephen M. Meckler,[§] Jonathan E. Bachman,[‡] Jeffrey R. Long,[‡,§,∥] and Brett A. Helms*,[†,∥]

[†]The Molecular Foundry, Lawrence Berkeley National Laboratory, 1 Cyclotron Road, Berkeley, California 94720, United States
[‡]Department of Chemical and Biomolecular Engineering, and [§]Department of Chemistry, The University of California, Berkeley, California 94720, United States
[∥]Materials Sciences Division, Lawrence Berkeley National Laboratory, Berkeley, California 94720, United States

Ⓢ *Supporting Information*

ABSTRACT: Despite the availability of chemistries to tailor the pore architectures of microporous polymer membranes for chemical separations, trade-offs in permeability and selectivity with functional group manipulations nevertheless persist, which ultimately places an upper bound on membrane performance. Here we introduce a new design strategy to uncouple these attributes of the membrane. Key to our success is the incorporation of phase-change metal−organic frameworks (MOFs) into the polymer matrix, which can be used to increase the solubility of a specific gas in the membrane, and thereby its permeability. We further show that it is necessary to scale the size of the phase-change MOF to nanoscopic dimensions, in order to take advantage of this effect in a gas separation. Our observation of an increase in solubility and permeability of only one of the gases during steady-state permeability measurements suggests fast exchange between free and chemisorbed gas molecules within the MOF pores. While the kinetics of this exchange in phase-change MOFs are not yet fully understood, their role in enhancing the efficacy and efficiency of the separation is clearly a compelling new direction for membrane technology.

KEYWORDS: *MOF nanocrystals, gas separations, mixed-matrix membranes, phase-change MOFs, CO$_2$/N$_2$ separations*
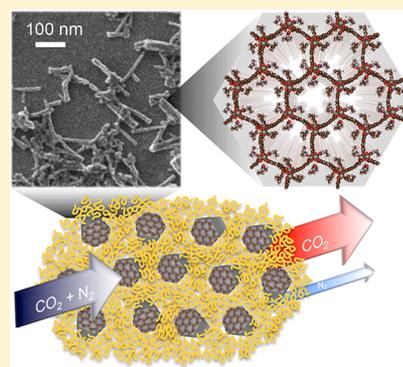
In the coming decades, climate change will likely lead to environmental and economic disruption.[1] Carbon dioxide, the primary greenhouse gas produced from the combustion of fossil fuels, is currently released into the atmosphere without mitigation at a rate of 36 Gton per year.[2] Carbon capture and sequestration has been proposed to reduce the amount of atmospheric CO$_2$. However, implementation of this technology necessitates low-cost and efficient methods for separating CO$_2$ from N$_2$ in a postcombustion capture process, where the carbon dioxide is removed from the effluent of power plants that burn coal or natural gas.[3] One of the most energy-efficient ways of capturing CO$_2$ is with a membrane-based separation.[4] Among the design platforms available for gas separation membranes, mixed-matrix membranes (MMMs) are promising: MMMs offer the low cost, high processability, and mechanical properties of polymers and, if successful, the unbounded separation performance of porous materials. Many MMMs overcome the intrinsic permeability-selectivity trade-off of pure polymers.[5,6] In recent years, zeolites and metal−organic frameworks (MOFs) have been used as fillers in MMMs[7−9] where typically molecular-sieving and solution-diffusion mechanisms[10] promote gas separation. In this work, we introduce for the first time a phase-change MOF,[11] mmen-Mg$_2$(dobpdc) (mmen = *N,N'*-dimethylethylenediamine; dobpdc$^{4−}$ = 4,4'-dioxidobiphenyl-3,3'-dicarboxylate, in a MMM to enhance the permeability and selectivity of CO$_2$ over N$_2$ (Figure 1).

While the use of mmen-Mg$_2$(dobpdc) as a CO$_2$ adsorbent and its associated thermodynamic underpinnings have been investigated thoroughly,[11−16] the kinetics of CO$_2$ transport in this phase-change material in a driven (i.e., out-of-equilibrium) system have not yet been reported; thus, their prospects for improving MMM-based gas separations are still unclear. It has been demonstrated that mmen-Mg$_2$(dobpdc) has a novel cooperative CO$_2$ uptake mechanism that leads to a nonclassical, steplike adsorption isotherm.[11] Having such a high, readily reversible CO$_2$ uptake makes the application of mmen-Mg$_2$(dobpdc) in membranes very attractive. Until now, attempts to incorporate this phase-change MOF in an MMM have failed, likely due to the dimensions of Mg$_2$(dobpdc) crystals obtained through conventional synthetic approaches; as shown in Figure S1, high aspect-ratio microrods, when blended with polymer, typically protrude from the matrix, which also appear to exhibit poorly formed polymer/MOF interfaces. To resolve issues associated with compositing larger MOF crystals,
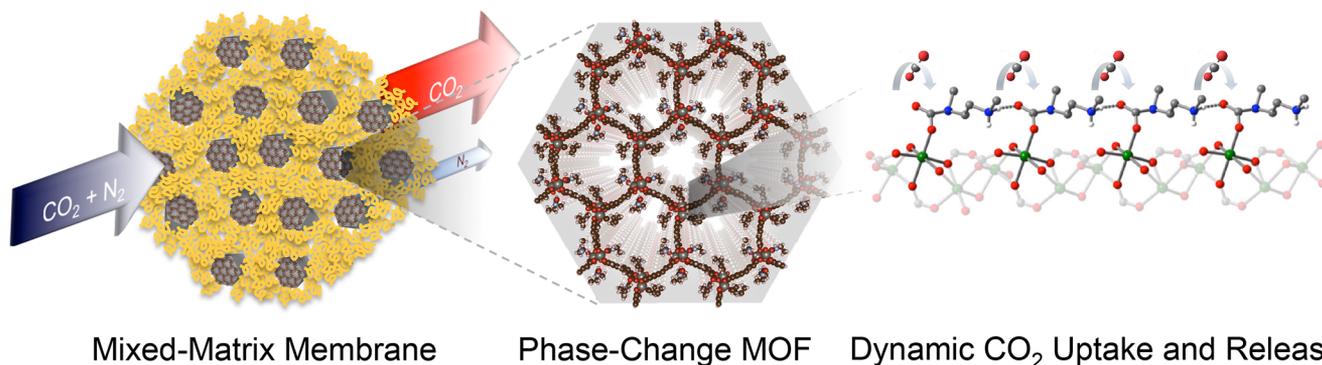
Figure 1. By incorporating phase-change MOFs in a mixed-matrix membrane, the permeability and selectivity for CO_2/N_2 separations can be greatly enhanced. Critical to the design of these composite membranes is the nanoscale dimension of the phase-change MOF filler, which serves to mitigate the effects of plasticization and likelihood of defects in the membrane that would negatively impact gas transport selectivity. Critical to the performance of the membranes is the dynamic uptake and release of CO_2 along the diamine molecules appended to open metal sites lining the MOF channels.
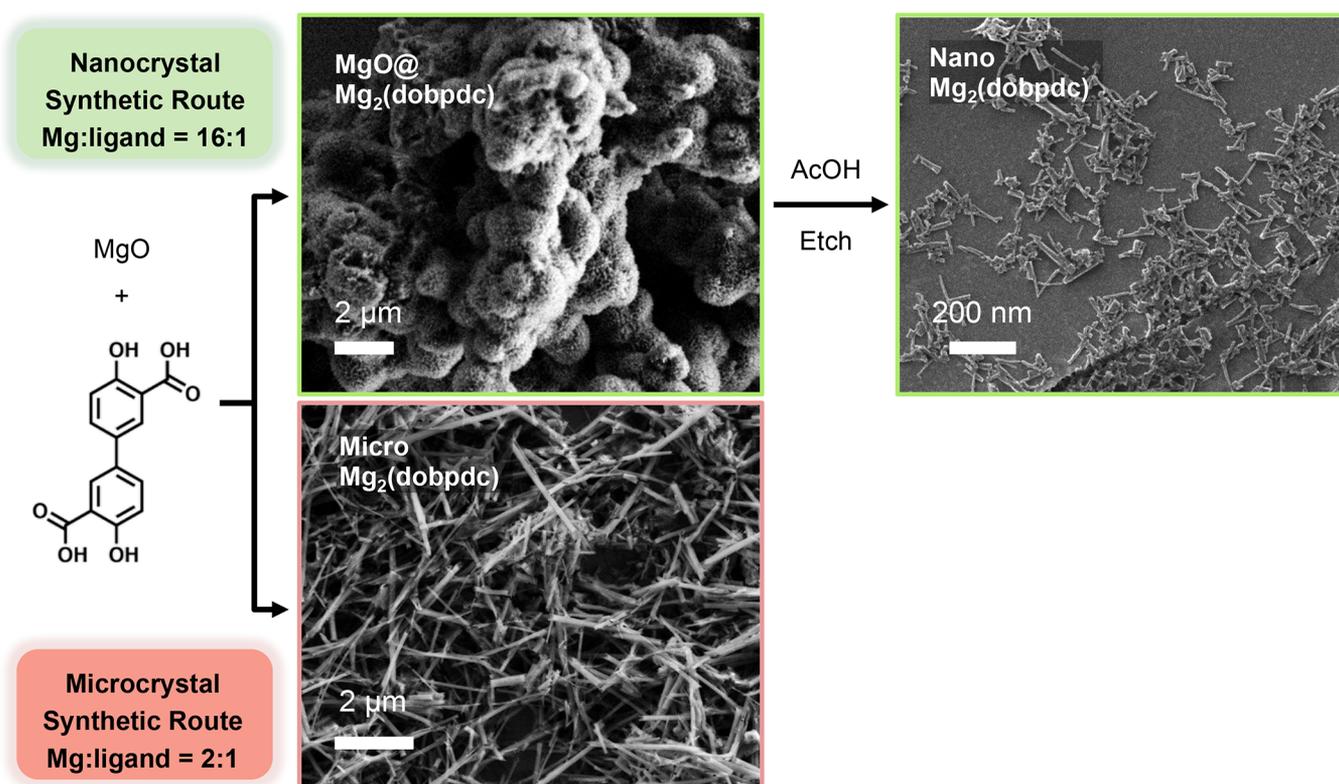

Figure 2. Varying the ratio of MgO to H_4dobpdc ligand during the chemical synthesis of Mg_2(dobpdc) MOFs allows the reaction coordinate to diverge, yielding either a forest of nanocrystalline MOFs on MgO solids or microcrystalline MOF rods. In the case of the former, the nanocrystalline MOFs can be released from the underlying MgO solids using acetic acid as a mild etchant. $Mg(OAc)_2$ byproducts are easily removed from the final nano-Mg_2(dobpdc) product.

we developed a new synthesis of Mg_2(dobpdc) nanocrystals. In turn, diamines were grafted within these Mg_2(dobpdc) nanocrystals to take advantage of their steplike CO_2 adsorptive properties in an MMM for CO_2/N_2 separations. With these new diamine-appended Mg_2(dobpdc) nanocrystals incorporated into MMMs, we find significant increases in CO_2 permeability while maintaining high CO_2/N_2 selectivity relative to the neat polymer matrix, essentially uncoupling conventional permeability-selectivity trade-offs typified by all-polymer membranes. This result points to new opportunities for MOF nanocrystals to enhance the performance of MMMs[9,17] and

encourages further investigation of other phase-change adsorbents as active components in gas-separation membranes.

To access Mg_2(dobpdc) nanocrystals for MMM preparation, we developed a new synthetic procedure with the goal of obtaining dispersible nanocrystals with properties similar to bulk crystals (Figure 2). We were ultimately successful by introducing the H_4(dobpdc) ligand to a superstoichiometric amount of MgO in DMF at 120 °C,[18] which generates a coating of Mg_2(dobpdc) nanorods on MgO. Precursor stoichiometry and reaction time were varied in turn to obtain Mg_2(dobpdc) nanorods with controlled morphology and length (e.g., 100–200 nm in size) (Figure 2). To isolate
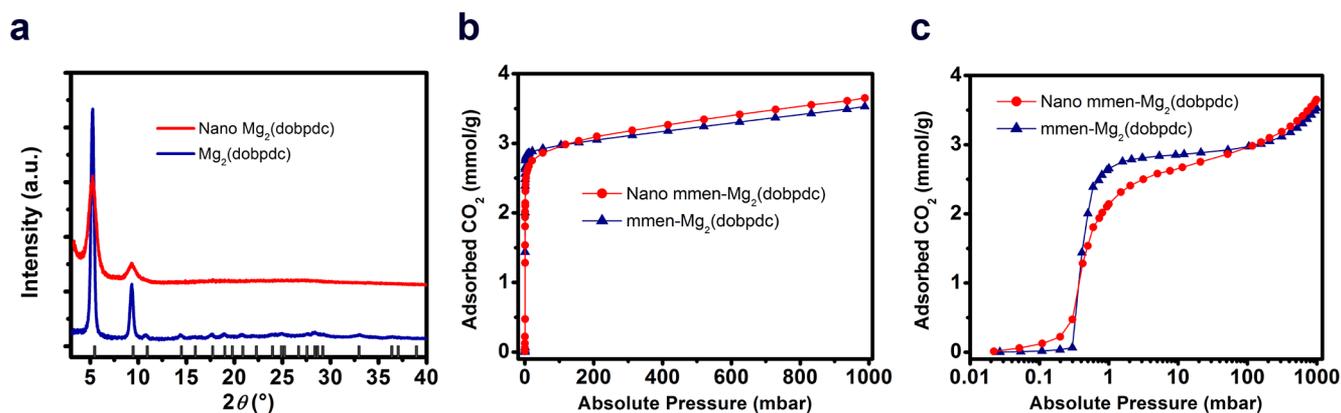
Figure 3. (a) PXRD of Mg$_2$(dobpdc) nanocrystals (red) and microcrystals (blue). In the nano-MOF sample, only high intensity peaks are visible and their fwhm is broader due to the small size of the crystallites. CO$_2$ adsorption isotherms of nanocrystalline (red) and microcrystalline (blue) mmen-Mg$_2$(dobpdc) in either (b) linear or (c) semilog plots. Saturation values are similar for both, while the adsorption step of mmen-Mg$_2$(dobpdc) nanorods is broader.

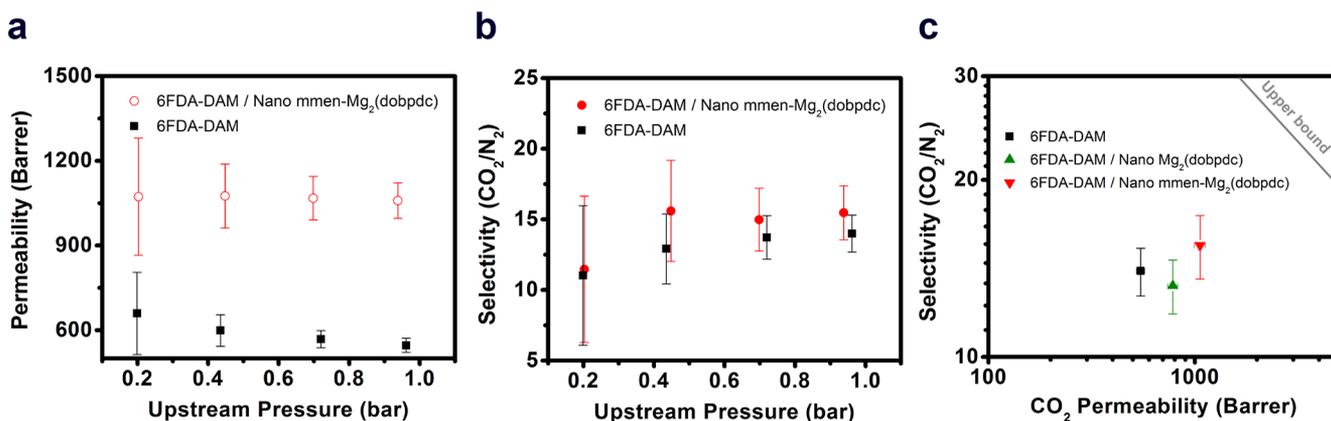**Figure 4.** Gas permeability measurements on neat 6FDA-DAM polymer (black) and 6FDA-DAM mixed-matrix membranes (red) with loaded with 23% *w/w* mmen-Mg$_2$(dobpdc) nanorods: (a) CO$_2$ permeability versus upstream pressure; and (b) CO$_2$/N$_2$ selectivity versus upstream pressure. Both CO$_2$ permeability and CO$_2$/N$_2$ selectivity increase in the MMM compared to the neat polymer. (c) Robeson plot for CO$_2$/N$_2$ separation showing performances of neat 6FDA-DAM (black), 6FDA-DAM mixed-matrix membranes incorporating Mg$_2$(dobpdc) nanorods (green), and 6FDA-DAM mixed-matrix membranes incorporating phase-change mmen-Mg$_2$(dobpdc) nanorods (red). The 2008 Robeson upper bound is plotted as a gray line.[24]

MOF nanorods, the MgO core was simply dissolved in acetic acid. The resulting purified MOF nanorods (Figure S3) were found to unaltered by the acetic acid treatment and they could be dispersed readily in polar aprotic solvents, such as DMF. Visualization of the reaction pathway is depicted in Figure S2. Notably, we found that higher Brunauer−Emmett−Teller (BET) surface areas (Figure S4a) and higher amine loadings (Figure S4b), were achieved after treating the nanorods in a subsequent step with H$_4$(dobpdc) in DMF at 120 °C, consistent with the presence of fewer defects in the final material.

Differences in the crystallinity of the Mg$_2$(dobpdc) nanorods compared to the micron-scale rods obtained from a bulk preparation are evident in Figure 3. Both experimental diffraction patterns match the calculated reflections for the crystal structure, and the peak broadening observed for the nano-MOF sample is consistent with the expected Scherrer broadening. Using Scherrer analysis, we estimate the crystallite size to be ∼12 nm, corresponding to the average nanorod cross-section. We further characterized the BET surface area for both samples (Figure S5), which unexpectedly revealed a greater surface area for the Mg$_2$(dobpdc) nanorods than for the

microrods. Deviations in behavior with regard to the shape of the N$_2$ isotherm manifests at high pressures, likely due to adsorption at surface sites, which are more prevalent in the nano-MOF.

To complete the preparation of the phase-change filler, *N,N′*-dimethylethylenediamine (mmen) molecules were grafted to the Lewis acidic open-metal sites within Mg$_2$(dobpdc) in toluene. No activation procedure was employed prior to diamine grafting, as we found drying to be detrimental to achieving good nanorod dispersions in the polymer matrix. After activating both nano- and micron-scale samples of mmen-Mg$_2$(dobpdc) MOFs at 100 °C, their CO$_2$ uptake was evaluated. The resulting adsorption isotherms are shown in Figure 3 as linear and semilog plots. The linear plot (Figure 3b) indicates CO$_2$ saturation capacity is quite comparable for the two crystal sizes, while the semilog plot (Figure 3c) reveals that the adsorption "step" of the mmen-Mg$_2$(dobpdc) nanorods is broader, corresponding to a lesser degree of cooperativity in the adsorption mechanism.[19] This could be due to finite-size effects in the formation of carbamate chains that are limited by the nanocrystal length or it could be the consequence of a higher number of mmen vacancies within the crystal. To put an upper

bound on the latter, thermogravimetric analysis (TGA) was carried out on nano- and micron-sized MOFs to quantify the mmen loadings. The results indicate a decrease in mmen loading within the nanorods of only 1.4% (Figure S6), which we believe to be negligible (i.e., within the experimental error).

To understand the influence of phase-change MOF fillers on membrane performance, we cast MMMs from a mixture of 6FDA-DAM polyimide and mmen-Mg_2(dobpdc) nanorods in dichloromethane. The quality of the dispersion was excellent, yielding transparent, flexible membranes after solvent evaporation. These membranes were tested in a custom-built, constant-volume, variable-pressure, gas-permeation apparatus. Permeabilities of N_2 and CO_2 were recorded and selectivities were calculated from the acquired data at different input (upstream) pressures. Both CO_2 permeability (Figure 4a) and CO_2/N_2 selectivity (Figure 4b) are greater in the MMM than in the neat polymer. To better clarify the role of the diamines inside the MOF, we prepared a membrane with bare Mg_2(dobpdc) nanorods within 6FDA-DAM and tested CO_2/N_2 permeation under the same conditions. The results, plotted in Figure 4c, are consistent with previous reports that showed that nano Mg_2(dobdc)/polymer MMMs outperform pure polymer membranes.[20] Figure 4c also shows that the diamines in mmen-Mg_2(dobpdc) nanorods significantly improve CO_2 permeability while also positively affecting CO_2/N_2 selectivity (Table S1).

We further performed gas permeation measurements on both 6FDA-DAM and mmen-Mg_2(dobpdc)−6FDA-DAM membranes (Figure S7) operating at higher temperatures (35−75 °C). We noted that the decrease in CO_2/N_2 selectivity with increasing temperature for the 6FDA-DAM membrane was significantly less pronounced than that for the mmen-Mg_2(dobpdc)−6FDA-DAM MMM. We expect that with increasing temperature, solubility and selectivity are reduced in both the neat polymer and in the MMM, with solubility playing a more pronounced role in the adsorbent-loaded material. Considering the temperature-dependent steplike character of CO_2 uptake and release that is the hallmark characteristic of the phase-change mmen-Mg_2(dobpdc) filler, adsorption sites within the MOF are left increasingly unoccupied at higher temperature, effectively decreasing the CO_2 solubility of the MMM. This effect dominates the steep decrease in CO_2/N_2 selectivity with increasing temperature in the MMM and corroborates our hypothesis that amine-appended MOFs primarily improve the performance of MMMs by increasing the CO_2 solubility. These data also suggest that the prevalence of interfacial polymer−MOF voids in the MMM is minimal or at least inconsequential.

On the basis of these results, we conclude that the diamines have an important role in the increase of CO_2 permeability and that this is likely related to the unique CO_2 cooperative adsorption behavior. We further speculate that selectivities could increase in real operating conditions, for example, in a mixed-gas environment. Indeed, under pure N_2, the transport is unaffected by CO_2 in the pore and we may expect higher N_2 permeability. Under a CO_2 environment, CO_2 can still transport down the channel while N_2 may be excluded due to the carbamate formation that effectively reduce the pore volume. We note that in absolute terms other polymers (e.g., polymers of intrinsic microporosity or thermally-rearranged polymers) can achieve superior performance in terms of CO_2 permeability, although their lack of stability over time has been a serious concern, preventing their use in industrial

applications.[21,22] MMMs are generally less susceptible to aging, and MOF nanocrystal−polymer composite membranes are resistant to plasticization.[17] Moreover, CO_2 adsorption is not affected by humidity in the amine-appended adsorbents,[21] unlike what is observed in metal−organic frameworks with bare metal sites.[22,23]

The presence of diamines in these phase-change MOF fillers could influence CO_2 and N_2 transport through several mechanisms, and the results presented here lend some insight into the relative impact of each. With diamines present in the MOF channel, the free diffusion of both gases is restricted due to the decrease in free volume relative to the bare framework. On the other hand, with diamines present CO_2 is chemisorbed strongly and selectively through the cooperative formation of ammonium carbamate chains; weak physisorption of either gas is still possible. Comparing the pressures used in the permeability measurements to the room-temperature CO_2 adsorption isotherm for a sample of mmen-Mg_2(dobpdc) nanorods suggests that ammonium carbamate formation should be highly favored throughout the membrane, since even the lower downstream pressure rapidly exceeds the 1 mbar adsorption threshold during the measurement. Because CO_2 saturation is measured at equilibrium, an increase in solubility, rather than diffusivity, more likely explains the increase in permeability. A detectable increase in solubility during steady-state permeability measurements suggests fast exchange between carbamate CO_2 and mobile CO_2 in the pores. To our knowledge, the kinetics of this exchange is not yet well understood, and our results thus motivate further study of the CO_2 dynamics in this system. A classical model of facilitated transport[25] captures some aspects of this system, but does not adequately describe the cooperative uptake. As N_2 does not participate in cooperative adsorption, its permeability is less dependent on the MOF chemical functionality and generally trends with free volume, which should be higher in the MMMs. Interestingly, the modest increase in selectivity upon the addition of diamines may be related to diamine pore-blocking impeding N_2 transport.

As further theoretical studies aimed at understanding out-of-equilibrium kinetics of CO_2 adsorption/desorption along the diamines emerge, our work presents the first validated guidepost as to their significance in phase-change MMM design rules. Our insights in that regard benefitted from pinhole free composites, which were only available when the particle dimensions were scaled to nanoscopic dimensions, introducing along the way a novel synthesis of Mg_2(dobpdc) nanorods based on kinetic control over the reaction coordinate. Our phase-change MMMs, when tested for CO_2/N_2 separation, yielded a 2-fold improvement in the CO_2 permeability, as well as a similarly high CO_2/N_2 selectivity, boding well for other membrane-based gas separations where the selector incorporates phase-change fillers.

■ ASSOCIATED CONTENT

Ⓢ Supporting Information

The Supporting Information is available free of charge on the ACS Publications website at DOI: 10.1021/acs.nanolett.7b03106.

Supporting Figures and Experimental Methods (PDF)

■ AUTHOR INFORMATION

Corresponding Author
*E-mail: bahelms@lbl.gov.

ORCID
Jonathan E. Bachman: 0000-0002-3313-2355
Jeffrey R. Long: 0000-0002-5324-1321
Brett A. Helms: 0000-0003-3925-4174

Author Contributions
The manuscript was written through contributions of all authors. All authors have given approval to the final version of the manuscript.

Notes
The authors declare no competing financial interest.

■ ABBREVIATIONS

mmen-Mg$_2$(dobpdc), mmen = N,N'-dimethylethylenediamine; dobpdc^{4-}, 4,4′-dioxidobiphenyl-3,3′-dicarboxylate; MMMs, mixed-matrix membranes; MOF, metal–organic frameworks

■ REFERENCES

(1) Revesz, R. L.; Howard, P. H.; Arrow, K.; Goulder, L. H.; Kopp, R. E.; Livermore, M. A.; Oppenheimer, M.; Sterner, T. *Nature* **2014**, *508*, 173−175.

(2) Jackson, R. B.; Canadell, J. G.; Le Quere, C.; Andrew, R. M.; Korsbakken, J. I.; Peters, G. P.; Nakicenovic, N. *Nat. Clim. Change* **2015**, *6*, 7−10.

(3) Smit, B.; Reimer, J. A.; Oldenburg, C. M.; Bourg, I. C. *Introduction to Carbon Capture and Sequestration*; World Scientific, 2014; Vol. 1.

(4) Angelini, P.; Armstrong, T.; Counce, R.; Griffith, W.; Klasson, T. L.; Muralidharan, G.; Narula, C.; Sikka, V.; Closset, G.; Keller, G. *DOE EERE Off. Wash. DC* **2005**, 103.

(5) Dong, G.; Li, H.; Chen, V. *J. Mater. Chem. A* **2013**, *1*, 4610−4630.

(6) Bastani, D.; Esmaeili, N.; Asadollahi, M. *J. Ind. Eng. Chem.* **2013**, *19*, 375−393.

(7) Rangnekar, N.; Mittal, N.; Elyassi, B.; Caro, J.; Tsapatsis, M. *Chem. Soc. Rev.* **2015**, *44*, 7128−7154.

(8) Koros, W. J.; Zhang, C. *Nat. Mater.* **2017**, *16*, 289−297.

(9) Ghalei, B.; Sakurai, K.; Kinoshita, Y.; Wakimoto, K.; Isfahani, A. P.; Song, Q.; Doitomi, K.; Furukawa, S.; Hirao, H.; Kusuda, H.; Kitagawa, S.; Sivaniah, E. *Nat. Energy* **2017**, *2*, 17086.

(10) Seoane, B.; Coronas, J.; Gascon, I.; Benavides, M. E.; Karvan, O.; Caro, J.; Kapteijn, F.; Gascon, J. *Chem. Soc. Rev.* **2015**, *44*, 2421−2454.

(11) McDonald, T. M.; Mason, J. A.; Kong, X.; Bloch, E. D.; Gygi, D.; Dani, A.; Crocella, V.; Giordanino, F.; Odoh, S. O.; Drisdell, W. S.; Vlaisavljevich, B.; Dzubak, A. L.; Poloni, R.; Schnell, S. K.; Planas, N.; Lee, K.; Pascal, T.; Wan, L. F.; Prendergast, D.; Neaton, J. B.; Smit, B.; Kortright, J. B.; Gagliardi, L.; Bordiga, S.; Reimer, J. A.; Long, J. R. *Nature* **2015**, *519*, 303−308.

(12) McDonald, T. M.; Lee, W. R.; Mason, J. A.; Wiers, B. M.; Hong, C. S.; Long, J. R. *J. Am. Chem. Soc.* **2012**, *134*, 7056−7065.

(13) Drisdell, W. S.; Poloni, R.; McDonald, T. M.; Pascal, T. A.; Wan, L. F.; Pemmaraju, C. D.; Vlaisavljevich, B.; Odoh, S. O.; Neaton, J. B.; Long, J. R.; Prendergast, D.; Kortright, J. B. *Phys. Chem. Chem. Phys.* **2015**, *17*, 21448−21457.

(14) Wu, D.; McDonald, T. M.; Quan, Z.; Ushakov, S. V.; Zhang, P.; Long, J. R.; Navrotsky, A. *J. Mater. Chem. A* **2015**, *3*, 4248−4254.

(15) Vlaisavljevich, B.; Odoh, S. O.; Schnell, S. K.; Dzubak, A. L.; Lee, K.; Planas, N.; Neaton, J. B.; Gagliardi, L.; Smit, B. *Chem. Sci.* **2015**, *6*, 5177−5185.

(16) Hefti, M.; Joss, L.; Bjelobrk, Z.; Mazzotti, M. *Faraday Discuss.* **2016**, *192*, 153−179.

(17) Bachman, J. E.; Smith, Z. P.; Li, T.; Xu, T.; Long, J. R. *Nat. Mater.* **2016**, *15*, 845−849.

(18) Maserati, L.; Meckler, S. M.; Li, C.; Helms, B. A. *Chem. Mater.* **2016**, *28*, 1581−1588.

(19) Weiss, J. N. *FASEB J.* **1997**, *11*, 835−841.

(20) Bae, T.-H.; Long, J. R. *Energy Environ. Sci.* **2013**, *6*, 3565.

(21) Mason, J. A.; McDonald, T. M.; Bae, T.-H.; Bachman, J. E.; Sumida, K.; Dutton, J. J.; Kaye, S. S.; Long, J. R. *J. Am. Chem. Soc.* **2015**, *137*, 4787−4803.

(22) Burtch, N. C.; Jasuja, H.; Walton, K. S. *Chem. Rev.* **2014**, *114*, 10575−10612.

(23) Kundu, J.; Pascal, T.; Prendergast, D.; Whitelam, S. *Phys. Chem. Chem. Phys.* **2016**, *18*, 21760−21766.

(24) Robeson, L. M. *J. Membr. Sci.* **2008**, *320*, 390−400.

(25) Cussler, E. L.; Aris, R.; Bhown, A. *J. Membr. Sci.* **1989**, *43*, 149−164.